

Pbar Note #695
 Signal Development for the Quadrupole BPM
 Vladimir Nagaslaev
 10 June 2004

I. Introduction.

We show here derivation for signal development in the Antiproton source quadrupole BPM. This is a quad pickup made of 1 m long electrostatic striplines. Each plate is connected to its own high impedance preamp mounted nearby and then output signals are going via long lines up to the service building. In order to suppress common mode, the preamps are designed as low frequency bandpass filters with maximum response at 10% of revolution frequency and 35 dB suppression of the first revolution harmonic. Thus the response is substantially nonuniform so both amplitude and phase corrections have to be made as signals at 3 different frequencies are involved. Cross-talk corrections have also been calculated.

II. Signal combinations.

A simple single pair pickup response is never exactly linear with the beam displacement. Leaving only first and second order terms voltage on plates in high preamp impedance approximation is:

$$V_{x\pm}(x, y) = ZI(t) \{1 \pm ax + b(x^2 - y^2)\} \quad (1a)$$

$$V_{y\pm}(x, y) = ZI(t) \{1 \pm ay - b(x^2 - y^2)\} \quad (1b)$$

where a and b are the pickup geometry parameters. Using 4 signals one can build linear combinations:

$$DX = X2 - X1 = V_{x+} - V_{x-} \propto a \langle x \rangle \quad (2a)$$

$$DY = Y2 - Y1 = V_{y+} - V_{y-} \propto a \langle y \rangle \quad (2b)$$

$$SX = X2 + X1 \propto 1 + b \langle x^2 - y^2 \rangle$$

$$SY = Y2 + Y1 \propto 1 - b \langle x^2 - y^2 \rangle \quad (3)$$

Combinations (2) are normally used in regular dipole pickups. Combinations 3 are not of a good use unless both are available at the same location. In case of a quadrupole pickup they are and combination

$$Q = SX - SY \propto b \langle x^2 - y^2 \rangle \quad (4)$$

gives access to the nonlinear term of pickup response and technique to measure bilinear beam characteristics. For instance, ellipticity $\sigma_x^2(t) - \sigma_y^2(t)$ can be used to determine the beam size or to observe quadrupole oscillations of the beam size. Following sections give more insight into this technique.

III. Frequency contents.

Let's consider transverse (horizontal in this notation) motion of an individual particle. Particle position is a sum of 3 components:

$$x_i = X_0 + X_\beta + \tilde{x}_i$$

X_0 - orbit position,

$X_\beta(t) = X_d \cos(\omega_r \nu_x t + \varphi_x)$ - coherent dipole (betatron) motion,

x_i - individual betatron motion with respect to the center of beam.

Putting this into (1a) and taking average over all particles in the beam we have

$$V_{x\pm}(t) = Z * I(t) \{ \quad (7)$$

$$1 + b * (X_0^2 - Y_0^2) + 0.5b * (X_d^2 - Y_d^2) \pm aX_0 + b * (\sigma_{0,x}^2 - \sigma_{0,y}^2) + \quad (I)$$

$$\pm aX_\beta(t) + 2b * (X_0 X_\beta(t) - Y_0 Y_\beta(t)) + \quad (II)$$

$$b * (X_\beta^2(t) - Y_\beta^2(t)) + b * (\sigma_{2,x}^2(t) - \sigma_{2,y}^2(t)) \} \quad (III)$$

This expression is broken up into 3 parts for convenience. “ \pm ” here corresponds to left and right (top and bottom) plates. Picking right signal combination one can effectively cancel contribution of symmetric or asymmetric components. Part (7-I) contains constant parameters, therefore it appears in signal as constant term and revolution harmonics. Looking at $S0 = SX + SY$ at revolution frequency and moving the beam center position one can find the value of b and the beam center position. The slope of DX plotted versus beam position would give value of a . Combination Q at revolution frequency can even be used to measure the beam size if electronics is calibrated at the level of better than 0.1%.

Part (7-II) contains linear amplitudes and mainly appears at betatron frequencies. DX and DY should give a clear dipole signal at betatron frequency.

Consequently, part (7-III) works at double betatron frequencies. It is clear that signal combination Q at this frequency is contributed by two sources,

$$Q^{(2)} = Qd + Qq$$

where Qq is a pure quadrupole signal and Qd is a nonlinear part of dipole signal. In general in order to get to Qq , one has to be able to do careful subtraction of Qd from measured signal Q .

IV. Imposing bunch structure of injected beam and response curve.

If $V(t)$ is the signal induced on the pickup plates, then the end signal received from the DAQ is its convolution with the response function of the electronics

$$U(t) = V(t) \otimes G$$

In frequency domain, we will present $G(w)$ for convenience, as $G=G_0g(w)$ with $g(w)$ being the frequency response function and G_0 - the general scale constant. For further convenience we will hide some other constants into G_0 , too. $V(t)$ here is a function of t described in eq.(7). Although Accumulator is designed to handle a DC beam, main area of quadrupole pickup applications is related to bunched beam operations, in particular at reverse proton injection, so we should treat in general $I(t)$ as a periodic function

$$I(t) = I_0 * \sum_n f(t - Tn), \quad \text{where } f(t) \text{ is a rectangular unit function.}$$

Let's consider part (7-I) in the simplest form $V(t) = Z * I(t)$. We have to take into account different revolution times for individual particles due to dispersion:

$$V(t) = I_0 Z \sum_n \overline{f(t - Tn)} = I_0 Z \sum_n \int dp \cdot \xi(p) f(t - T(p)n)$$

$\xi(p)$ is a momentum distribution in the beam. Because this is a periodic structure, it can be expanded in harmonic series. In order to find coefficients we use the following trick:

The Fourier image for the signal is:

$$V_w(\omega) = I_0 Z \int dt \cdot e^{i\omega t} \sum_n \int dp \cdot \xi(p) f(t - nT(p)) = I_0 Z \sum_n \int dp \cdot \xi(p) e^{i\omega nT(p)} \tau \cdot s\left(\frac{\omega\tau}{2}\right)$$

here $s(x)=\sin(x)/x$, τ is an incoming bunch train duration. Using the property

$$\sum_n e^{ian} = 2\pi \sum_k \delta(a - 2\pi k), \text{ we get}$$

$$V_w(\omega) = 2\pi \bar{I} Z s\left(\frac{\omega\tau}{2}\right) \sum_n \int dp \cdot \xi(p) \delta(\omega - n\omega_r(p))$$

Now conversion back to time is also simple:

$$V(t) = \bar{I}Z \sum_n \int dp \cdot \xi(p) \int d\omega \cdot e^{-i\omega t} \delta(\omega - n\omega_r(p)) s\left(\frac{\omega\tau}{2}\right)$$

Presenting $\omega_r(p)$ as $\omega_0(1 + \eta \frac{p}{P_0})$, rewrite

$$V(t) = \bar{I}Z \sum_n s\left(\frac{n\omega_0\tau_0}{2}\right) e^{-in\omega_0 t} \int dp \cdot \xi(p) e^{-i\frac{\omega_0 n \eta}{P_0} p} = \bar{I}Z \sum_n s\left(\frac{n\omega_0\tau_0}{2}\right) e^{-in\omega_0 t} F\left(\frac{\omega_0 n \eta}{P_0} t\right)$$

$F(x)$ here is the Fourier transform for the momentum distribution function. Obviously, the width of this function is smaller for higher harmonics. And now coupling this with the response function, we arrive at the expansion for the “common mode” signal:

$$U(t) = 2G_0 \bar{I} \sum_{n=1}^{\infty} g(\omega_0 n) s\left(\frac{\omega_0 n \tau}{2}\right) * \left| F\left(\frac{n\eta}{P_0} \omega_0 t\right) \right| \cos(\omega_0 n t + \varphi_n) \quad (8)$$

Note that argument in s -function has a meaning: $\frac{n\omega_0\tau_0}{2} = n\pi \frac{N_b}{h}$, where N_b is a number of bunches in an injected train and h is a total rf harmonic number for the ring.

For terms like (7-II) we use the same trick and obtain:

$$V(t) = g(\omega_r v_x) * G_0 I(t) * \cos[\omega_r v_x t + \varphi_x] \rightarrow$$

$$U_n(t) = g(\omega_0 |v_0 \mp n|) * G_0 \bar{I} * \left[\frac{\sin\left(\frac{\omega_0 n \tau}{2}\right)}{\left(\frac{\omega_0 n \tau}{2}\right)} \cos[\omega_0 (v_0 \mp n)t + \varphi_x + \delta_{n,\pm}] * \left| F\left(\frac{C_x - \eta(v_0 \pm n)}{P_0} \omega_0 t\right) \right| \right] \quad (9)$$

where

$$F\left(\frac{C_x - \eta(v_0 \pm n)}{P_0} \omega_0 t\right) = \left| F\left(\frac{C_x - \eta(v_0 \pm n)}{P_0} \omega_0 t\right) \right| * e^{i\delta_{n,\pm}}$$

Here we had to take into account chromaticity C_x .

And similarly, decomposition into series for functions of the (7-III) type is

$$\begin{aligned}
V(t) &= g(\omega_r \nu_x) * G_0 I(t) * \cos^2(\omega_r \nu_x t + \varphi_x) \quad \rightarrow \\
U_n(t) &= \frac{1}{2} G_0 \bar{I} \cdot s \left(\frac{\omega_0 n \tau}{2} \right) \left\{ 2g(\omega_0 n) \left| F \left(\frac{n\eta}{P_0} \omega_0 t \right) \right| \cos(\omega_0 n t + \varphi_0) + \right. \\
&\quad \left. + g(\omega_0 |2\nu_0 \mp n|) \left| F \left(\frac{2C - \eta(2\nu_0 \pm n)}{P_0} \omega_0 t \right) \right| \cos \left(\omega_0 (2\nu_0 \mp n)t + 2\varphi_x + \delta_{2,n,\pm} \right) \right\} \quad (10)
\end{aligned}$$

Obvious properties of $F(x)$:

$$\begin{aligned}
F(x) &\cong 1, \\
\delta_{2,n,\pm} &\cong 0 \quad \text{when } x \ll \frac{1}{\Delta p}
\end{aligned}$$

$$\delta_{2,n,\pm} = 0 \quad \text{if } f(p) \text{ is symmetric.}$$

It can be clearly seen that at high chromaticity signal decays quickly due to decoherence of oscillation signal. Another conclusion from equations 8-10 is that signal is strongly dominated by the common mode component (8), unless properly filtered.

V. Calculation of geometric parameters and their frequency dependence (cross-talk).

In case of infinite preamplifier input impedance beam with charge Q_b would induce potential at the i -th plate

$$\varphi_{i\infty}(x, y) = a(i, x, y) * Q_b$$

and when beam is exactly at the center, $\varphi_{i\infty}(0,0) = V_0$

for small compared to aperture deviations of beam from the center, induced potential may be approximated as

$$\varphi_{i\infty}(x, y) = V_0 * \{1 \pm a_0 * x + b_0 * (x^2 - y^2)\}$$

geometric coefficients a_0 , b_0 can be computed from the electrostatic model of BPM. This was done using MERMAID program. Obtained response signal combinations DX and Q are shown in Figure 1 as functions of pick-up position.

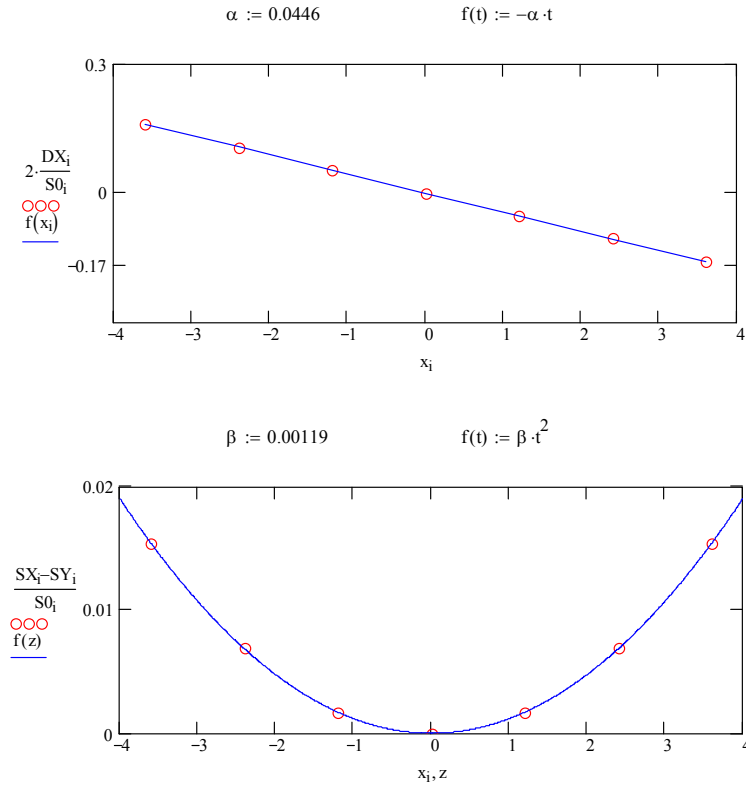


Figure 1. Induced signal on the plates as function of PU position.

Now let's take into account the preamp's impedance at finite frequency, see Figure 2.

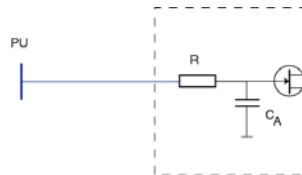


Figure 2. Input impedance of the QBPM preamplifier.

As in our case $C_A \cong C_d$, effective parallel capacitance significantly changes at low frequencies.

$$\varphi_{i,w}(x, y) = \varphi_{i,\infty}(x, y) + S_{ik} * q_k,$$

where $[S_{ik}] = [C_{ik}]^{-1}$, inverse capacitance matrix. The meaning of this equation is the following: at low frequencies input impedance may be considered very high, and the total charge on the pickup plates remain zero. At higher frequencies this is not so

anymore, because impedance becomes smaller. This charge results in changing the potentials on plates (cross-talk). Solving this equation yields:

$$\varphi_{i,w}(x, y) = \left[\delta_{ik} + \frac{C_A}{1 + i\omega RC_A} S_{ik} \right]^{-1} \varphi_{k\infty}(x, y) \quad (11)$$

and coefficients \mathbf{a} and \mathbf{b} become frequency dependent.

The capacitance matrix was calculated in framework of the same program. Setting on the right plate such a charge that its potential is 1V (this is not necessary, and was done for convenience of computations only), see Figure 3, we calculate potential on other plates.

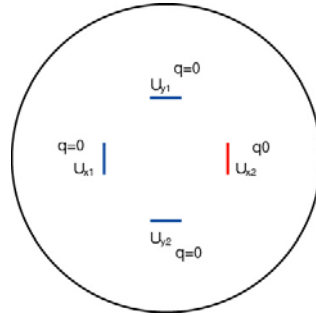


Figure 3. Computation of the cross-capacitance matrix.

$$S_i = V_i / q_0 = \begin{bmatrix} 5.708 \cdot 10^{-3} \\ 0.04625 \\ 0.1582 \cdot 10^{-3} \\ 0.1582 \cdot 10^{-3} \end{bmatrix}$$

Now we can reconstruct the whole matrix using its symmetry:

$$\begin{aligned} S_{12} &= S_{21} = S_{34} = S_{43} = S_{i_1} \\ S_{13} &= S_{31} = S_{14} = S_{41} = S_{32} = S_{23} = S_{42} = S_{24} = S_{i_3} \\ S_{11} &= S_{22} = S_{33} = S_{44} = S_{i_2} \end{aligned}$$

and now using eq. (11) we can calculate dependence $\mathbf{a}(f)$ and $\mathbf{b}(f)$, as shown in Figure 4.

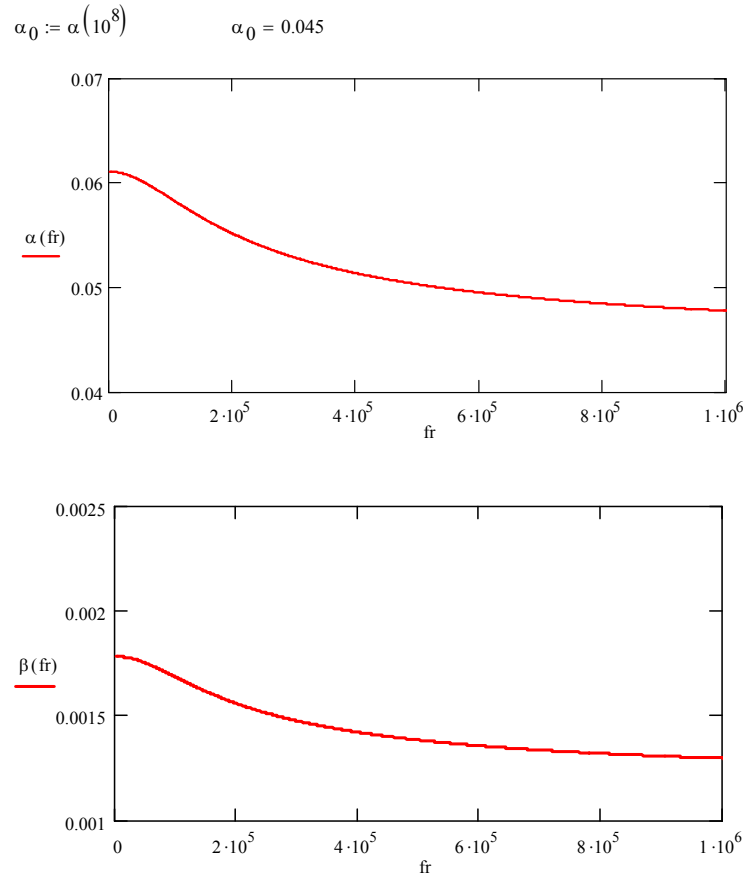


Figure 4(a,b). Calculated dependence $a(f)$ and $b(f)$

The measured and calculated parameters are compared in Table 1. Table also contains parameters a_0 and b_0 measured in beam position scans. There is a very good agreement with the horizontal scan. For reasons not yet fully understood at this moment vertical scan doesn't agree very well with the horizontal one.

Table 1. The calculated and measured geometric parameters.

	Model, $f = \infty$	Model, $f = f_0$	Horz. meas.	Vert. meas.
a	0.0450	0.0493	0.0498	0.0455
b	0.00119	0.00135	0.00132	0.00146

VI. Application to measurements.

As it has been pointed out earlier, quadrupole oscillations decohere quickly if the chromaticity is high. This is the case for the extraction orbit in Accumulator. For this reason real measurements require modifications in preamplifiers. This is being addressed presently, meanwhile benchmark dedicated measurements were done with artificially lowered chromaticity.

We set up injection with a large dipole mismatch, so that the quadrupole signal is completely dominated by the dipole component Q_d , in this case we should be able to determine this component based on the dipole signal measured at single betatron frequency.

We can rewrite amplitudes of known signal combinations according to eq. (8-10):

$$S_0 = 8g_0G_0\bar{I} \frac{\sin\left(\frac{\omega_0\tau}{2}\right)}{\left(\frac{\omega_0\tau}{2}\right)} \quad (12)$$

$$DX_0^{(1)} = \frac{a_1}{4} X_d \frac{g_1}{g_0} S_0 \quad (13)$$

$$Q_0^{(2)} = \frac{b_2}{4} \frac{g_2}{g_0} S_0 X_d^2 = 4 \frac{b_2}{a_1^2} \frac{g_2 g_0}{g_1^2} \frac{DX_0^2}{S_0} \quad (14)$$

where $a_1 = a(\omega_0(1-\nu_x))$, $b_2 = b(\omega_0(2\nu_x - 1))$, upperscript (1) and (2) in eq.(13,14) denote single and double betatron frequency. It seems convenient to tie amplitudes with parameter K_f , which can be independently determined from both measurements and calculations:

$$\frac{DX_0^{(1)}}{S_0} = X_d \cdot K_f, \quad K_f = \frac{a_1}{4} \cdot \frac{g_1}{g_0}$$

$$Q_0^{(2)} = \frac{b_2}{a_1} \frac{g_2}{g_1} \frac{1}{K_f} \frac{DX_0^2}{S_0}$$

using parameters \mathbf{a} , \mathbf{b} calculated in previous sections, we expect the dipole term in the quadrupole signal to have the form:

$$Qfc(t) = Q_0^{(2)} e^{-\frac{2t^2}{\sigma^2}} \cos(2\pi \cdot f_0(2\nu_x - 1)t + \phi_1 + \phi_{PA})$$

Here time decay constant σ and phase ϕ_1 are taken from the dipole mode fit, and ϕ_{PA} is the phase advance between single and double betatron frequency in the preamp response.

03/31/03

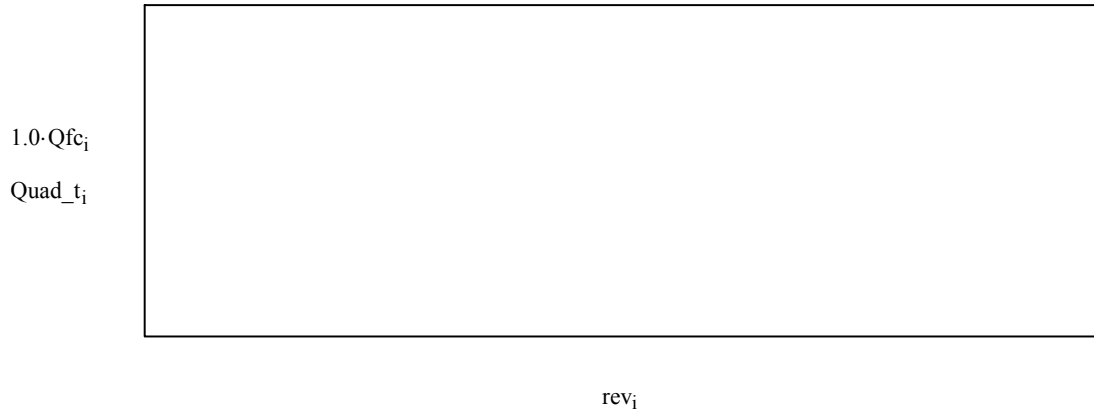


Figure 9. Measured and calculated dipole component in quadrupole signal

Not only the amplitude, expected phase fits measured signal nicely, which verifies the calculations performed above. Another setup was to make betatron mismatch dominant, measured quadrupole signal is compared with calculated Qd in Fig. 10:

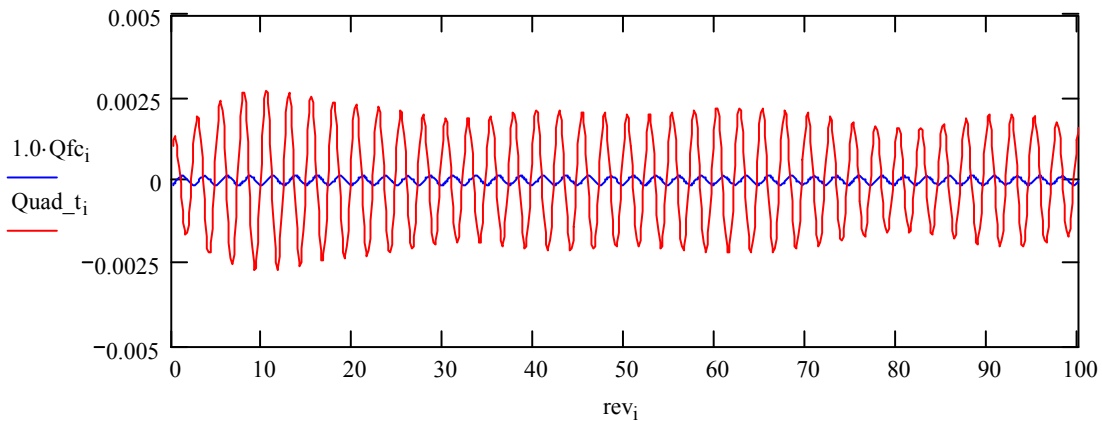


Figure 10. Pure quadrupole oscillation signal in absence of dipole component. Beats are artifacts of aliasing due to frequency cuts applied on measured signal.

The dipole component is negligible and quadrupole oscillation signal is clearly seen although its amplitude is low. Parasitic components at revolution and betatron frequencies were removed from the $Quad_t$ signal, this was done by filtering a broad region around double betatron frequency in FFT spectrum of Q signal combination and then deconvolving this region back to time domain. This explains aliasing modulations of

the signal sin-wave. Observed amplitude of quadrupole oscillation is consistent with the introduced betatron mismatch assuming $\varepsilon_{beam} = 16\pi$ for injected Reverse proton beam, and corresponds to emittance growth of 50%.

VII. Conclusions.

We presented here formulae derivation for calculations of signals in the quadrupole Accumulator BPM. Electrostatic model was used to compute the geometry parameters for this pick-up as well as their frequency dependence (cross-talk effect). Obtained relations between signals at single and double betatron frequency were examined and have shown a good agreement with direct measurements.